

Investigating the effect of rainfall patterns on slope stability through physical and numerical modelling

J. Peranić¹, A. Leonard², L. Kocijančić¹, Ž. Arbanas¹

¹*University of Rijeka, Faculty of Civil Engineering, Radmile Matejčić 3, 51000 Rijeka, Croatia*

²*Institut Polytechnique de Grenoble, 46 avenue Felix Viallet, 38031 Grenoble Cedex 01, France*

ABSTRACT: This study examines the impact of rainfall patterns on the hydraulic response and stability of a sandy slope model. Laboratory experiments were conducted on a 35° slope model instrumented with soil moisture and suction probes and exposed to constant, increasing, and decreasing rainfall patterns, each delivering the same totally infiltrated water volume. The role of initial soil moisture was also investigated under a constant intensity of 80 mm/h. Results show that rainfall patterns and initial conditions significantly influence soil moisture and suction evolution, yet no deformations or signs of failure were observed in any test. To complement the experiments, numerical simulations were carried out to replicate the hydraulic processes, followed by limit equilibrium stability analyses. Preliminary results highlight some distinct trends in how rainfall patterns affect hydraulic behaviour and slope stability. These findings form part of a broader ongoing research project aimed at exploring additional soil types, including fine-grained soils, and more complex rainfall patterns. The work contributes to advancing understanding of rainfall-driven slope responses—an increasingly critical topic under changing climate conditions.

Keywords: landslides; rainfall infiltration; physical modelling; numerical modelling; unsaturated soil

1 INTRODUCTION

Soil moisture and pore water pressure (pwp) conditions within vadose zone of slopes result from a complex interplay among soil, vegetation, and atmosphere. The hydraulic response of a slope to rainfall depends on many factors, including rainfall characteristics and soil properties. While numerous studies have investigated the effects of total infiltrated volumes and established the relationships between rainfall intensity, duration, and the occurrence of rainfall-induced landslides, recent studies have highlighted that rainfall patterns themselves can play a decisive role in infiltration dynamics, moisture redistribution, and slope stability under unsaturated conditions (e.g., Fan et al., 2020; Zheng and Or, 2020).

Numerical parametric studies examining various rainfall patterns—such as normal, advanced, delayed, or cyclic—have demonstrated that the Factor of Safety (FoS) and slope stability responses vary according to the temporal distribution of rainfall. Mohammad et al. (2024) found that clayey soil slopes subjected to cyclic or advanced rainfall patterns tend to exhibit higher stability compared with those experiencing delayed or continuous rainfall, primarily due to differences in the timing and magnitude of pwp increases. Furthermore, the reduction in the Fos was generally more pronounced for gentler slopes under advanced rainfall and for steeper slopes under delayed rainfall patterns, illustrating the interaction between slope geometry and precipitation timing (Jamel et al., 2025; Fathiyah and Erly, 2017).

This study integrates physical and numerical modelling, two well-established approaches for investigating rainfall-induced landslide phenomena and related processes (e.g., Cuomo and Della Sala, 2013; Kristo et al., 2017; Peranić et al., 2021, 2022; Yang et al., 2021), to examine the comparative effects of different rainfall patterns—constant, increasing, and decreasing—under an equal total infiltrated volume. The experiments were designed to ensure identical drying times, thereby minimizing the influence of initial moisture distribution on the results. The experimentally collected data are used to evaluate the impact of simulated rainfall conditions on the evolution of pwp and volumetric water content in the sandy slope model, as well as on the overall slope stability condition.

This contribution presents a selected portion of a broader ongoing research project aimed at exploring additional soil types, including fine-grained soils, and more complex rainfall scenarios, with the objective to enhance understanding of how different rainfall patterns affect the hydraulic response and stability of a sandy slope model, and to assess the suitability of the adopted experimental and numerical methodologies for investigating such phenomena.

2 METHODOLOGY

The physical model setup, testing conditions, and details of the digital twin model and numerical analyses performed are presented in this section.

2.1 Physical modelling setup

The physical modelling tests were conducted at the Geotechnical Laboratory of the University of Rijeka, Faculty of Civil Engineering, within the framework of several ongoing research projects. The experimental setup included the platform for testing slope models exposed to simulated rainfall under 1g loading conditions, the rainfall simulator and the comprehensive monitoring system that allows monitoring the hydraulic and mechanical response of the model. While the monitoring of the onset of displacements, both surficial and within the slope model, mostly relies on accelerometers, laser scanning, digital image correlation and photogrammetry (Figure 1), the focus of the presentation is on theta probes and mini-tensiometers: a part of the geotechnical monitoring network that enable monitoring changes in soil moisture and suction (as well as positive pwp) throughout the test.

2.1.1 Building and preparation of the soil

The uniformly graded fine sand, characterized by a 35° friction angle and basic physical and hydraulic properties reported in Table 1, was compacted in five layers within the 1m wide platform, to obtain 35° inclined slope model 0.3 m thick, ensuring uniform initial density with targeted porosity of 0.44 (l) and moisture content of 2% (in gravimetric terms) with-in the model as much as possible. A 5 cm gravel drainage layer was placed beneath the base-type sandy soil to prevent the groundwater level rise and bottom-up slope saturation, i.e., to enable observation of the depth-limited model's response in partially saturated conditions during infiltration. A thin geosynthetic separator was placed between the sand and gravel layers to prevent migration and washing out of finer sandy particles in the coarse layer below. Considering that the main motivation of the experiment was to observe changes in soil moisture and pwp under different simulated rainfall conditions, some downscaled gabion wall elements were applied in the lowest part of the model to improve the model's foot stability during different rainfall scenarios. Figure 2 presents the physical slope model at the end of the construction stage.

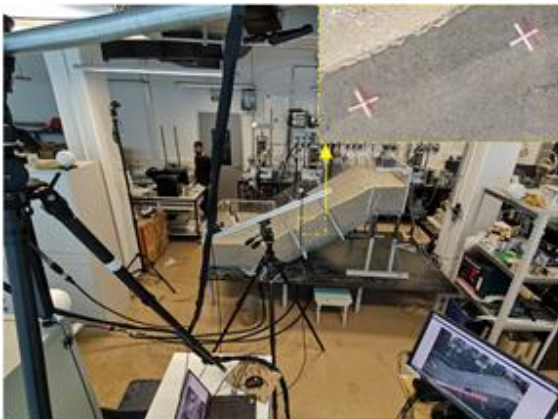


Figure 1. The ARAMIS system (GOM mbH) comprising of two pairs of high-speed stereo cameras.

Table 1. Basic physical and hydraulic properties of the uniformly graded sand encompassed in the study

Parameter	Symbol (unit)	Value
Specific gravity	G_s	2.7
Particle sizes	D_{10} (mm)	0.19
	D_{60} (mm)	0.37
Min/max void ratio	e_{min}/e_{max}	0.64/0.91
Saturated hydraulic cond.	k_s (m/s)	$3.3e-04$
van Genuchten's SWCC parameters	α (kPa)	0.82
	n	2.7

2.1.2 Slope instrumentation

After the model was built, vertical cuts were made for the instrumentation of the slope with 18 sensors, distributed along three vertical profiles as shown in Figure 3 (upper – I_U , middle – I_I , and lower – I_L). Each profile included sensors installed at depths of 6 cm, 12 cm, 18 cm, and 24 cm measured normal to the slope surface. Soil moisture was monitored using TEROS 10 and TEROS 12 probes (METER Group Inc.), while pwps were recorded with mini-tensiometers TEROS 31, capable of measuring both positive and negative pwp in the range from +50 to –85 kPa. The sensors were connected to ZL6 data loggers, allowing continuous data acquisition during and after rainfall application. Special care was taken during installation to minimize soil disturbance and ensure good hydraulic contact between the sensors and surrounding material. For example, soil compaction was avoided during insertion to preserve target porosity, and mini-tensiometers were exposed to air only briefly during installation.

2.1.3 Rainfall simulation, experimental procedure and instrumentation

A custom-built rainfall simulator allows the control of rainfall intensity, duration, and distribution uniformity. The system consists of three adjustable arms, each equipped with four different full-cone axial nozzles (Lechler 490 series, 60° spray angle), positioned to uniformly cover the model. The operational pressure range (0.5–4 bar) allows rainfall intensities between approx.. 20 mm/h and 200 mm/h. Water pressure and flow were regulated through a control block including reduction valves, flowmeters, and electromagnetic solenoid valves, enabling automation and repeatability of the experiments (more details in Peranić et al., 2022).

In total, four tests were performed, each of them lasting for 60 minutes of rainfall simulation with the same cumulative volume of rainfall delivered to the model of 80 litres. Each test was followed by a 24-hour drying period before the next experiment, in order to establish almost identical initial moisture content as suction profiles, thus enabling the direct comparison of observed responses. Testing procedure was as follows:

- **Test 0** (Constant intensity): the test with a constant rainfall intensity of 80 mm/h, which followed the model construction stage with relatively dry conditions;



Figure 2. A 35° model built from uniformly-grained fine sand over a 5 cm thick layer of gravel.

- **Test 1** (Increasing intensity): rainfall increased stepwise every 15 minutes, from 20 to 140 mm/h;
- **Test 2** (Constant intensity): rainfall kept constant at 80 mm/h throughout the test; and
- **Test 3** (Decreasing intensity): rainfall was reduced stepwise from 140 to 20 mm/h in 15-min intervals.

2.2 Numerical modelling setup

The transient rainfall infiltration and slope stability analyses were performed using Slide2 (Rocscience Inc.) software. A digital twin of the slope was constructed based on the previously described material properties, geometry, and boundary conditions. The underlying drainage layer was modelled assuming a hydraulic conductivity of $k_s = 0.01$ m/s, with saturated and residual volumetric water contents of 0.4 and 0.0, respectively. Other relevant parameters were adopted as representative values for gravel and, according to parametric numerical analyses, had negligible influence on the overall computational outcomes.

Slide2 employs the finite element method to integrate Richards' equation, thereby obtaining the soil moisture and pwp distributions resulting from the transient infiltration process. The domain was discretized using approximately 3,500 three-noded triangular elements. The model was initialized through steady-state analyses, with suction of 4.6 kPa applied uniformly across the domain, consistent with experimental observations (Figures 4&5). The transient analysis comprised 60 time steps, each lasting one minute. Pwp distributions

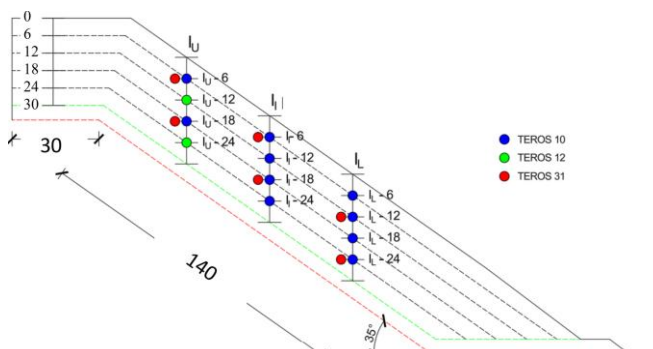


Figure 3. Measurement profiles with soil and pwp sensors. Green and red dotted lines represent the sand/gravel interface and the impermeable bottom, respectively

obtained every five minutes were stored, and the FoS was computed using the limit equilibrium method for circular sliding surfaces with the auto-refine search option. For brevity, only the results obtained using the Morgenstern–Price method are presented, focusing on the global minimum safety factor values.

3 RESULTS AND INTERPRETATION

This presentation provides the results obtained for the shallowest monitored points (6 cm depth) across all three branches and Tests 1, 2, and 3. Figure 5 shows the measured soil moisture and pwp over the 60-minute rainfall and the subsequent 60-minute drainage phase.

The results revealed a consistent relationship between the evolution of soil-moisture content and pwp. In all tests, the volumetric water content increased rapidly within the first 10–15 minutes, followed by a gradual stabilization phase. The corresponding pwp exhibited a delayed response, typically 3–5 minutes after the increase in water content. While in-depth analysis is beyond the scope of this presentation, it is worth outlining that the lowest profile showed different response, likely due to lateral unsaturated flow or other phenomena.

In Test 1, the rise in water content was slowest, but the peak values were the highest. The maximum volumetric water content reached $\theta = 0.366$ m³/m³ at 24 cm depth (profile I_U), with a minimum suction of $u_w \approx -0.53$ kPa (I_L– 24 cm). In Test 2, the maximum water content was slightly lower ($\theta \approx 0.338$ m³/m³) with $u_w \approx -0.76$ kPa, clearly indicating the establishment of steady-state infiltration under constant rainfall intensity. Test 3 produced a rapid initial wetting but lower ultimate values ($\theta \approx 0.336$ m³/m³, $u_w \approx -0.63$ kPa) due to decreasing intensity and enhanced drainage toward the slope toe.

The time required for the wetting front to reach the shallowest sensor (6 cm depth) also varied: approximately 10 minutes for Test 1, 9 minutes for Test 2, and 7 minutes for Test 3. Although these confirm that higher initial rainfall intensities accelerate infiltration through the unsaturated sand layer, full saturation was not achieved in any of the tests. The corresponding slope stability analysis results are presented in Figure 6.

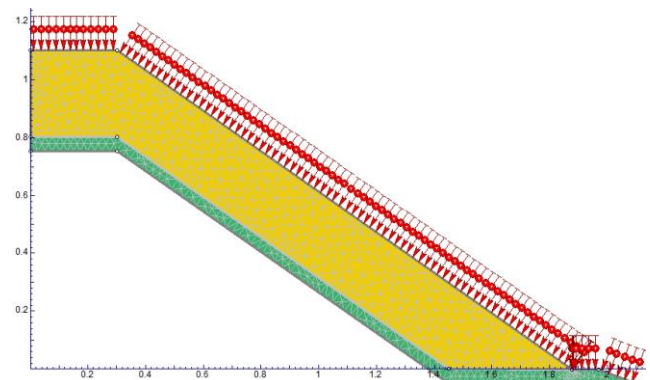


Figure 4. Digital twin build in Slide2 (Rocscience Inc.) programme with applied boundary conditions and 3-noded triangles used for the discretization of the domain

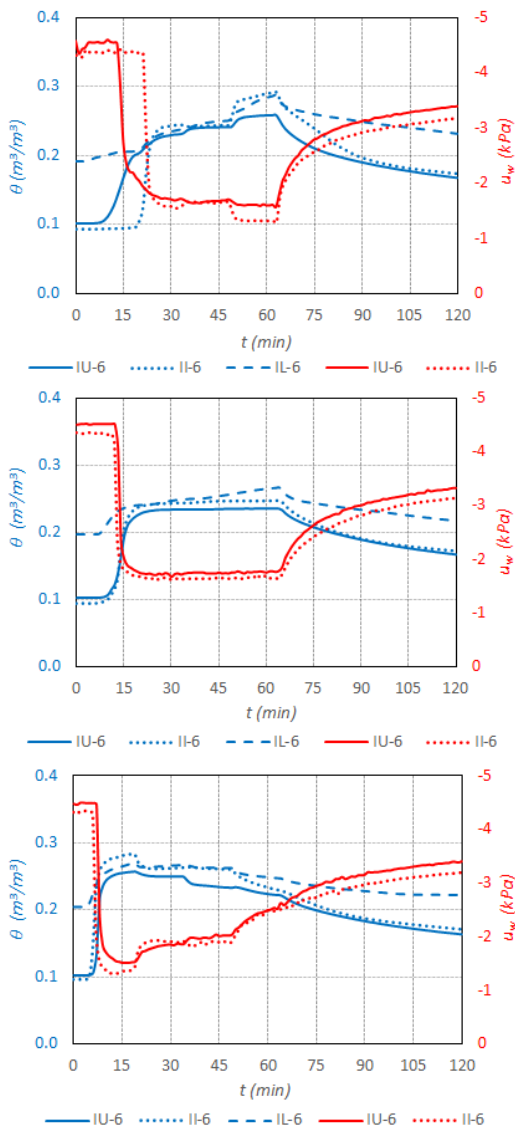


Figure 5. Soil moisture (blue) and pore pressure (red) changes in Test 1 (top), Test 2 (middle), Test 3 (bottom)

4 CONCLUSIONS

A rapid rise in soil moisture and pwp was observed within the first minutes of the experiment for the decreasing rainfall pattern, whereas changes were smoother and more delayed for the increasing pattern. However, after approximately 45 min, the increasing pattern exhibited a sharp rise in volumetric water content. The steady pattern followed an intermediate trend. Consequently, the evolution of the FoS also differed among the three cases (Figure 6): the increasing-intensity rainfall pattern produced the most adverse conditions, resulting in both the greatest increase in moisture and PWP, as well as the lowest FoS value. When comparing with depth, it was found that decreasing-intensity rainfall tends to produce more uniform and rapid wetting, while the increasing pattern leads to a stronger temporal lag with depth. This highlights the influence of rainfall pattern on internal hydraulic gradient dynamics, which in turn control slope stability.

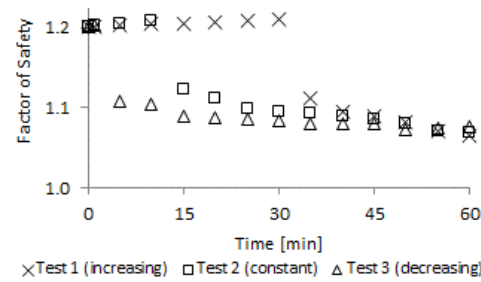


Figure 6. The global minimum factor of safety values for the three tests calculated with Slide2 (Rocscience Inc.)

It is worth noting that, probably due to the nature of the tested soil, the differences among the cases were relatively small. Further investigations are therefore needed to draw more definitive conclusions: it is expected that less permeable slopes would exhibit greater differences in hydraulic and stability behaviour.

5 ACKNOWLEDGMENTS

This research has been supported by the University of Rijeka and the International Consortium on Landslides through the uniri-iskusni-tehnic-23-240, uniri-iz-25-208 and IPL-256 projects. These supports are gratefully acknowledged.

6 REFERENCES

- Crescenzo, L., Peranić, J., Arbanas, Ž., Calvello, M. 2024. An approach to calibrate the unsaturated hydraulic properties of a soil through numerical modelling of a small-scale slope model exposed to rainfall, *Acta Geotechnica* **19**, 4437–4456.
- Cuomo, S., Della Sala, M. 2013. Rainfall-induced infiltration, runoff and failure in steep unsaturated shallow soil deposits, *Engineering Geology* **162**, 118–127.
- Fathiyah, H.S., Erly B. 2017. Parametric study on the effect of rainfall pattern to slope stability. *MATEC Web of Conf.: Sriwijaya Int. Conf. on Eng. S&T (SICEST 2016)* (Eds: Iskandar, I., Ismadji, S., Agustina, T.E., Yani, I., Komariah L.N. & Hasyim, S.), 101, 05005. EDP Sciences.
- Jamel, A.A.J. 2025. The Effect of Rainfall Intensity on Slope Stability: An Analytical Study using Numerical Modeling, *Engineering, Technology & Applied Science Research* **15**(2), 21203–21207.
- Kristo, C., Rahardjo H., Satyanaga, A. 2017. Effect of variations in rainfall intensity on slope stability in Singapore, *International Soil and Water Conservation Research* **5**(4), 258–264.
- Peranić, J., Mihalić Arbanas, S., Arbanas, Ž. 2021. Importance of the unsaturated zone in landslide reactivation on flysch slopes: observations from Valići Landslide, Croatia, *Landslides* **18**, 3737–3751.
- Peranić, J., Čeh, N., Arbanas, Ž. 2022. The Use of Soil Moisture and Pore-Water Pressure Sensors for the Interpretation of Landslide Behavior in Small-Scale Physical Models, *Sensors* **22**(19), 7337.
- Yang, K.H., Nguyen, T.S., Rahardjo, H., Lin DG. 2021. Deformation characteristics of unstable shallow slopes triggered by rainfall infiltration, *BOEG* **80**, 317–344.